

**SYNTHESIS OF SINGLE-WALL CARBON NANOTUBE VIA CVD GROWTH
MECHANISM**

LIU WEI WEN

**UNIVERSITI SAINS MAALYSIA
2011**

**SYNTHESIS OF SINGLE-WALL CARBON NANOTUBE VIA CVD GROWTH
MECHANISM**

by

LIU WEI WEN

**Thesis submitted in fulfillment of the requirements
for the degree of
Doctor of Philosophy**

September 2011

ACKNOWLEDGEMENTS

My most sincere appreciation is forwarded to my main, Assoc. Prof. Dr. Azizan and co-supervisor, Prof. Dr. Abdul Rahman Mohamed, for being an excellent mentor, giving me the most valuable guidance. They just like the candle giving light to me so that I know where I should heading. I would like to appreciate Prof. Dr. Abdul Rahman Mohamed for giving the chance to me to do my project using his carbon nanotubes production rig, testing equipments, other facilities in MTDC lab and grant to covers most of the expenses of my project. I also would like to thanks Dr. Tye Ching Thian, my co-supervisor, for providing invaluable criticisms and guidance during my studies.

I would like to thank Prof. Ahmad Fauzi b. Mohd Noor, Dean of the School of Materials and Mineral Resources Engineering USM, Prof. Hanafi b. Ismail and Assoc. Prof. Dr. Azhar b. A bu Bakar, Deputy Deans of the School of Materials and Mineral Resources Engineering, for their continuous motivation, cultivated briefing on t he postgraduate project and showing helpful in postgraduate affairs throughout my studies. I would like to extend my sincere appreciation to all lecturers in this school for giving me support and guidance.

I would like to express my gratitude to all the laboratory technicians and administrative staff of the School of Materials and Mineral Resources Engineering and School of Chemical Engineering, for their kind assistance rendered to me. A special appreciation I want to give is Madam Fong, senior technician from School of Materials and Mineral Resources Engineering, Mr. Pachamuthu and Madam Faizah of the School of Biological Science, their assistance will always being remembered.

I also would like to give thank to some friends: Dr. Chai Siang Piao, Dr. Derek Chan, Khe, Pi Lin, Pek Ling, See Yao, Jeremy, Sam, Hock Jin, Way Fong, Wei Ching, Kenneth, Xiao Mei, Kelvin Ng, Moon See, Trung, Cao Xuan Viet, Le Min Hai, Khang, Warapong, Yi Jing, Wei Ling, Melissa Tung, Pei Ching, Dr. Low Siew Chun, Dr. Sim Jia Huey, Thiam Leng, Mun Sing, Lee Pu Min, Teh Kian Teck, Tang Yeng Hok and others whom I always remember.

I am indeed grateful to my parents and siblings. They are always giving me encouragement and moral support. Lastly, I am very much indebted to the MOSTI and Universiti Sains Malaysia for providing me the financial support under Fundamental Research Grant Scheme (FRGS) (Project: A/C No: 6071002) and Research University Postgraduate Research Grant Scheme (RU-PRGS) (Project: A/C No: 8042015). I also would like to Universiti Sains Malaysia for giving me the USM Fellowship scholarship for three years.

Thank You.

Liu Wei Wen

September 2011

TABLE OF CONTENTS

	Page
AKNOWLEDGEMENTS	ii
TABLE OF CONTENTS	iv
LIST OF TABLES	vii
LIST OF FIGURES	ix
LIST OF ABBREVIATIONS	xiv
LIST OF SYMBOLS	xvi
ABSTRAK	xvii
ABSTRACT	xviii
CHAPTER 1 - INTRODUCTION	1
1.1 Nanomaterials	1
1.2 Carbon nanotubes	2
1.3 Synthesis of SWCNTs	4
1.4 Growth mechanism of SWCNTs	5
1.5 Problem statement	7
1.6 Research objectives	9
1.7 Scope of the study	10
CHAPTER 2 - LITERATURE REVIEW	12
2.1 Introduction of carbon nanotubes	12
2.1.1 Discovery of carbon nanotubes	12
2.1.2 Structure of CNTs	14
2.1.3 Properties and application of carbon nanotubes	16
2.2 Synthesis of carbon nanotubes	20
2.2.1 Arc-discharge	20
2.2.2 Laser ablation	21
2.2.3 Chemical vapour deposition	22
2.3 Catalyst preparation methods	23
2.3.1 Sol-gel method	23
2.3.2 Coreduction of precursors	24
2.3.3 Impregnation	24
2.3.4 Ion-exchange-precipitation	24
2.4 Catalyst used for CNT growth	25
2.5 Physical and chemical state of the catalyst	27
2.6 Effect of reaction temperature	29
2.7 Effect of reaction time	32
2.8 Effect of carbon precursor and carrier gas flow rate	34
2.9 Effect of type of carrier gas	35
2.10 Effect of type of carbon precursor	37
2.11 Models of catalytic growth in chemical vapour deposition	39
2.12 Can single-walled carbon nanotubes grow on non-catalyst surface?	45
2.13 Catalytic growth mechanism for SWCNTs	46
2.14 Catalytic growth mechanism for SWCNT bundles	51
2.15 Base-growth mechanism for SWCNTs	52

2.16	The question remains in the growth mechanism for CNTs	53
2.17	Principle of experimental design	55
2.17.1	Two level factorial design (2^k)	57
2.17.2	Response surface methodology (RSM)	57
2.17.3	Central composite design (CCD)	58
2.17.4	Validation of model adequacy	59
2.17.5	Coefficient of determination (R^2)	59
2.17.6	Residual analysis	60
2.17.7	Lack of fit	60
2.18	Optimisation of operating conditions for SWCNTs using RSM and Factorial design	61
CHAPTER 3 - MATERIALS AND METHODS		64
3.1	Materials and chemicals	64
3.1.1	Chemicals	64
3.1.2	Gases	64
3.2	Experimental rig diagram	65
3.3	Selection of catalyst system	66
3.4	Synthesis of Fe_3O_4 nanoparticles and Fe_3O_4/MgO catalyst	68
3.5	Selection of Al_2O_3 , SiO_2 and MgO as catalyst support	69
3.6	Determination active metal loading on the MgO support	70
3.7	Optimisation of reaction conditions for SWCNT production	70
3.7.1	The path of experiment design	70
3.7.2	Model fitting and statistical analysis	71
3.7.3	Model equation development	71
3.8	Determination of mechanism of CNTs growth	73
3.8.1	Experimental	74
3.9	CNTs and catalyst characterisation	77
3.9.1	Raman spectroscopy	77
3.9.2	Thermogravimetric analysis (TGA)	78
3.9.3	Scanning electron microscopy (SEM)	79
3.9.4	Transmission electron microscopy (TEM)	80
3.9.5	X-ray diffraction (XRD)	81
3.9.6	Gas chromatography mass spectrometry (GCMS)	82
CHAPTER 4 - RESULTS AND DISCUSSION		83
4.1	Design of catalyst to synthesise single-walled carbon nanotubes	83
4.1.1	Synthesis of Fe_3O_4 nanoparticles	83
4.1.2	Selection of catalyst system	83
4.1.3	Selection of Al_2O_3 , SiO_2 and MgO as catalyst supports	90
4.1.4	Determination of active metal loading on the MgO support	97
4.1.5	Characterization of Fe_3O_4/MgO catalyst system	105
4.2	Optimisation of reaction conditions for the synthesis of SWCNTs using response surface methodology	109
4.2.1	Model equation development	110
4.2.2	Model evaluation	111
4.2.3	Residual analysis	112

4.2.4 Effect of reaction temperature, reaction time and reaction gas flow rate on the I_D/I_G ratio and presence of RBM peaks	117
4.2.5 Effect of reaction temperature, reaction time and reaction gas flow rate on the carbon weight and presence of RBM peaks	136
4.2.6 Process optimisation	144
4.2.7 Characterisation of SWCNT under optimum conditions	145
4.3 Mechanism of CNT formation	145
4.3.1 Growth of CNTs from benzene at 600, 700, 800, 900 and 1000°C	149
4.3.2 Growth of CNTs from camphor at 600, 700, 800, 900 and 1000°C	155
4.3.3 The comparison of growth mechanism between methane and benzene	164
4.3.4 Effect of molecular structure of carbon precursor on CNTs quality	168
4.3.5 Comparison diameter of SWCNTs between methane and benzene samples.	171
4.3.6 Distributions of metallic and semiconducting CNTs produced by methane and benzene.	174
CHAPTER 5 - CONCLUSIONS	179
CHAPTER 6 - RECOMMENDATIONS FOR FUTURE RESEARCH	182
BIBLIOGRAPHY	183
APPENDICES	201
APPENDIX A Calculation of diameter and carbon weight	202
APPENDIX B GCMS Chromatograph Data	203
APPENDIX C GCMS Chromatograph Data	204
APPENDIX D GCMS Chromatograph Data	205
APPENDIX E GCMS Chromatograph Data	206
APPENDIX F GCMS Chromatograph Data	207
APPENDIX G XRD Spectrum	208
LIST OF PUBLICATIONS	209

LIST OF TABLES

		Page
Table 2.1	Three models of growth mechanism that have been proposed until recently.	56
Table 3.1	List of chemical used and its brand	64
Table 3.2	Active metal loading on the support in molar ratio.	70
Table 3.3	Experimental design matrix for SWCNT production	73
Table 4.1	I_D/I_G ratio for carbon product produced by different active metal.	88
Table 4.2	I_D/I_G ratio for the Al_2O_3 , SiO_2 and MgO supported catalysts.	91
Table 4.3	Active metal loading on the support in molar ratio.	98
Table 4.4	Experimental design matrix for SWCNT production.	113
Table 4.5	Model summary statistics of I_D/I_G ratio model.	114
Table 4.6	Model summary statistics of carbon weight model.	114
Table 4.7	Analysis of ANOVA for response surface quadratic model for I_D/I_G .	115
Table 4.8	Analysis of ANOVA for response surface quadratic model for carbon weight.	115
Table 4.9	Calculated values of I_D/I_G ratio and presence of RBM peaks.	118
Table 4.10	Comparison of the I_D/I_G ratio for run 6-11 and 13-14.	130
Table 4.11	Calculated values of carbon weight and presence of RBM peaks.	138
Table 4.12	Model predicted and experimental values of I_D/I_G ratio, carbon weight and presence of RBM peaks for optimised process conditions (reaction temperature, reaction time and reaction gas flow rate).	144
Table 4.13	Various kinds of possible aromatic carbon molecules detected at different retention time.	155
Table 4.14	Comparison of the proposed growth mechanism of CNTs produced by different types of catalysts at different temperature range.	166

Table 4.15 Calculated area of ω_{met}^- and ω_{semi}^- peaks for methane and benzene samples.

178

LIST OF FIGURES

	Page
Figure 1.1	The structure of SWCNT (Nanodimension, 2005). 3
Figure 2.1	Structure of the buckminsterfullerene (C_{60}). 13
Figure 2.2	The structure of (a) graphite, (b) diamond. 14
Figure 2.3	CNT formed by rolling up a graphite sheet (Andrews, 2006). 15
Figure 2.4	Structures of (a) single-wall, (b) double-wall, (c) multi-wall CNTs (Burstein, 2003). 15
Figure 2.5	A diagram of arc-discharge setup (Saito <i>et al.</i> , 1998). 20
Figure 2.6	A diagram of laser ablation setup (Yakobson and Smalley, 1997). 21
Figure 2.7	A diagram of CVD setup (Lee <i>et al.</i> , 2002). 23
Figure 2.8	(a) Base-growth model of nanotube. (b) Tip-growth model of nanotube. 40
Figure 2.9	The proposed ring addition mechanism of nanotube growth from benzene. The benzene molecules are absorbed on the catalyst surface and followed by dehydrogenation of benzene molecules and formation of graphene (Andrews, 2006). 43
Figure 2.10	Schematic of a transition metal surface decorated fullerene (C_{60}) inside a open-ended carbon (white spheres) nanotube. The Ni and Co atoms (large dark spheres) adsorbed in between the C_{60} surface and nanotube wall are possible agents to help in building the length of nanotube (Birkett <i>et al.</i> , 1997). 47
Figure 2.11	The metal catalyst (large black sphere) keeps the nanotube (white ball-and-stick atomic structure) open by “scooting” around the open edge. This will ensure that any pentagons or other high energy local structures are arranged to hexagons (Thess <i>et al.</i> , 1996a). 48
Figure 2.12	The growth of a armchair SWCNT (Hamada <i>et al.</i> , 1992). The low coordinated carbon atoms (dangling bonds) are represented as light grey spheres on the top of tube (left). 49

Figure 2.13	Schematic of a nanotube bundle consists of seven armchair SWCNTs (white spheres) (Guo <i>et al.</i> , 1995). Some transition metal catalyst atoms (black) are occupying sites between the growing edge of adjacent of nanotubes for stabilization.	52
Figure 2.14	TEM image for SWCNTs growing vertically from a Ni-carbide particle (bottom) (Qin and Iijima, 1997). The top inset illustrates the growth process of SWCNTs from a metal-carbide particle: (a) segregation of carbon towards the surface, (b) nucleation of SWCNTs on the particle surface, and (c) formation of SWCNTs (Saito <i>et al.</i> , 1994).	54
Figure 3.1	Schematic of the experimental rig.	64
Figure 3.2	Flow chart of CVD in the production of CNTs.	67
Figure 3.3	Strategy of experimentation.	72
Figure 3.4	Diagram of CVD setup. Benzene was heated on a hot plate in a conical flask.	75
Figure 3.5	Diagram of CVD setup for study CNT production using camphor.	76
Figure 3.6	A SEM image showing vertical aligned CNTs (Cao <i>et al.</i> , 2002)	80
Figure 3.7	High-magnified TEM images of CNTs grown on un reduced catalyst (Chai <i>et al.</i> , 2007)	81
Figure 3.8	Chromatogram for an alpine snow sample (Santos and Galceran, 2003)	82
Figure 4.1	(a) TEM image of Fe ₃ O ₄ nanoparticles. (b) Histogram showing the diameter distribution of Fe ₃ O ₄ nanoparticles. (c) HRTEM image of Fe ₃ O ₄ nanoparticles.	84
Figure 4.2	Raman spectra of CVD products of (a) NiO/MgO (b) CoO/MgO and (c) Fe ₃ O ₄ /MgO catalyst.	88
Figure 4.3	Bundles of SWCNTs produced by (a) NiO/MgO (b) CoO/MgO and (c) Fe ₃ O ₄ /MgO catalyst.	89
Figure 4.4	Raman spectra of CVD products of (a) SiO ₂ supported catalyst (b) Al ₂ O ₃ supported catalyst, and (c) MgO supported catalyst.	92
Figure 4.5	SEM images of samples produced by (a) SiO ₂ supported catalyst (b) Al ₂ O ₃ supported catalyst, and (c) MgO supported catalyst.	94

Figure 4.6	TEM images of SWCNT bundles synthesised by (a) Al ₂ O ₃ supported catalyst (b) SiO ₂ supported catalyst.	96
Figure 4.7	Raman spectra of CVD products of (a) (Fe ₃ O ₄) ₁ (MgO) ₉ catalyst (b) (Fe ₃ O ₄) _{1.75} (MgO) _{8.25} catalyst, (c) (Fe ₃ O ₄) _{2.5} (MgO) _{7.5} catalyst and (d) (Fe ₃ O ₄) _{3.25} (MgO) _{6.75} catalyst.	99
Figure 4.8	SEM images of the CVD product produced by (a) (Fe ₃ O ₄) ₁ (MgO) ₉ catalyst (b) (Fe ₃ O ₄) _{1.75} (MgO) _{8.25} catalyst, (c) (Fe ₃ O ₄) _{2.5} (MgO) _{7.5} catalyst and (d) (Fe ₃ O ₄) _{3.25} (MgO) _{6.75} catalyst.	100
Figure 4.9	TEM image of samples produced by (a) (Fe ₃ O ₄) ₁ (MgO) ₉ catalyst. (b) (Fe ₃ O ₄) _{1.75} (MgO) _{8.25} catalyst (c) (Fe ₃ O ₄) _{2.5} (MgO) _{7.5} catalyst (d) (Fe ₃ O ₄) _{3.25} (MgO) _{6.75} catalyst .	104
Figure 4.10	(a) Low-magnified and (b) high-magnified TEM images of Fe ₃ O ₄ nanoparticles supported on MgO. (c) EDX analysis of the Fe ₃ O ₄ /MgO catalyst. (d) HRTEM image of the Fe ₃ O ₄ /MgO catalyst.	106
Figure 4.11	XRD patterns of (a) Fe ₃ O ₄ nanoparticles (b) the Fe ₃ O ₄ /MgO catalyst.	109
Figure 4.12	Predicted vs. experimental (a) I _D /I _G , and (b) carbon weight.	116
Figure 4.13	(a), (b), (c), and (d) Raman spectra of the CNTs synthesised at different temperatures for run 1-5, 6-10, 11-15 and 16-20, respectively.	119
Figure 4.14	One-factor plot of reaction temperature.	121
Figure 4.15	Catalyst used in CVD at (a) 329°C, (b) 500°C	123
Figure 4.16	Melting temperature of selected metals as a function of particle diameter (Moisala <i>et al.</i> , 2003).	124
Figure 4.17	(a) Growth of nanotubes at 750°C. (b) The 1000°C sample showed a dense growth of highly-graphitised nanotubes over its surface. (c) Large and low graphitisation degree of CNTs were observed growing over the catalyst at 1170°C. (d) TEM image for CNTs produced at 1170°C.	126
Figure 4.18	One-factor effect of reaction time on I _D /I _G ratio.	131
Figure 4.19	TEM images and EDX analysis for CNTs samples produced at (a) 20 min. (b) 45 min. (c) 70 min.	133

Figure 4.20	One-factor effect of reaction gas flow rate on I_D/I_G ratio.	134
Figure 4.21	Interaction effects between parameters of reaction temperature and gas flow rate.	136
Figure 4.22	TGA analysis for catalyst reacted at (a) 329 and (b) 500°C.	139
Figure 4.23	One-factor plot reaction temperatures showing the effect of reaction temperature on the carbon weight.	141
Figure 4.24	One-factor plot reaction time, showing the effect of reaction time on the carbon weight.	142
Figure 4.25	One-factor plot of the effect of reaction gas flow rate on the carbon weight.	143
Figure 4.26	(a) SWCNTs prepared under optimum conditions. (b) HRTEM image of SWCNT bundle grown under optimum conditions. (c) Thermal analysis of the carbon sample prepared under optimum conditions. (d) Raman spectrum of SWCNTs formed under the optimum conditions.	146
Figure 4.27	Molecular structures for (a) camphor (b) benzene (c) methane (Andrews, 2006).	148
Figure 4.28	TEM images of the benzene CVD product produced at (a) 600°C, (b) 700°C, (c) 800°C, (d) 900°C and (e) 1000°C.	152
Figure 4.29	Raman spectra of samples produced using benzene at different temperatures.	154
Figure 4.30	Chromatogram for gas sample collected at (a) benzene standard, (b) 1000°C, (c) 900°C, (d) 800°C, (e) 700°C, and (f) 600°C.	157
Figure 4.31	SEM images of CVD product using camphor as carbon precursor and produced at (a) 600°C (b) 700°C (c) 800°C (d) 900°C and (e) 1000°C.	158
Figure 4.32	Raman spectra of CVD product using camphor as carbon precursor at different temperatures.	160
Figure 4.33	XRD patterns for CVD products produced using camphor at different temperatures.(*). Fe_3O_4/MgO .	161
Figure 4.34	Chromatogram for gas sample collected at (a) 1000°C, (b) 900°C, (c) 800°C, (d) 700°C, and (e) 600°C.	165

Figure 4.35	Molecular structure of (a) $C_{10}H_8$ and (b) $C_{14}H_{28}$.	166
Figure 4.36	A proposed growth model of formation graphene on c atalyst surface. The white circle is carbon atom.	167
Figure 4.37	The ring addition mechanism proposed for the formation of CNTs from benzene (Tian <i>et al.</i> , 2003).	168
Figure 4.38	(a) TEM image (b) Raman spectra of the samples produced from methane and benzene.	170
Figure 4.39	RBM peaks of the Raman spectra of the methane and benzene.	172
Figure 4.40	Diagram of the CNT growth mechanism by benzene and methane.	174
Figure 4.41	G bands for (a) samples from benzene (b) samples from methane.	177

LIST OF ABBREVIATIONS

CNFs	Carbon nanofibers
CNTs	Carbon nanotubes
CVD	Chemical vapour deposition
GCMS	Gas chromatography
HRTEM	High-resolution transmission electron microscopy
RBM	Radial breathing mode
RSM	Response surface methodology
SEM	Scanning electron microscopy
SWCNTs	Single-wall carbon nanotubes
TEM	Transmission electron microscopy
TGA	Thermogravimetric analysis
VLS	Vapor-liquid-solid
XRD	X-ray diffraction
STM	Scanning Tunneling Microscopy
MWCNTs	Multi-wall carbon nanotubes
HiPCO	High-pressure catalytic decomposition of carbon monoxide
PECVD	Plasma-enhanced chemical vapor deposition
FET	Field effect transistor
HRO	Hard-to-reduce oxide
CCD	Central composite design
OFAT	One-factor-at-a-time
PCS	Polycarbosilane

PE	Polyethylene
CVD-FBR	Chemical vapour deposition-fluidized bed reactor
DWCNTs	Double-wall carbon nanotubes
MSI	Metal support interaction
ANOVA	Analysis of variance
AAD	Absolute average deviation
SSE	Error sum of squares
SST	Total sum of squares
DOE	Design of Experiment
EDX	Energy dispersive X-ray
RT	Retention time

LIST OF SYMBOLS

R^2	Coefficient of determination, defined by $R^2 = 1 - (SSE/SST)$
Y	Predicted response
b_0	Constant coefficient
b_i	Linear coefficients
b_{ij}	Interaction coefficients
b_{ii}	Quadratic coefficients
x	Coded values
r_i	Residual
\hat{Y}_i	Experimental value
Y_i	Calculated value from the model
n	Replicate
α	Alpha value
n_c	Center runs

SINTESIS KARBON NANOTIUB DINDING TUNGGAL MELALUI MEKANISME PERTUMBUHAN CVD

ABSTRAK

Karbon nanotub dinding tunggal (SWCNTs) telah dikaji dan dihasilkan sejak 1993 oleh ramai penyelidik. Salah satu cabaran ialah memartabatkan mekanisme pertambahan gelang untuk julat suhu tindak balas yang lebar. Dengan ini, mekanisme pertumbuhan SWCNTs yang dihasilkan daripada hidrokarbon dapat difahami dengan sepenuhnya. Maka ini menjadi tumpuan utama kerja ini. Kajian ini dimulakan dengan pembangunan sistem mangkin yang dapat menghasilkan SWCNTs bermutu tertinggi daripada penguraian metana. Kaedah permukaan respons (RSM) telah digunakan untuk mengoptimumkan parameter tindak balas seperti suhu tindak balas, masa tindak balas dan kadar aliran gas tindak balas. Keadaan optimum untuk menghasilkan SWCNTs dengan kualiti tinggi telah ditentukan sebagai: suhu tindak balas 900°C, masa tindak balas 59 minit dan kadar aliran (metana/nitrogen) gas tindak balas 54 ml/min. Kesan sumber karbon ke atas sintesis (karbon nanotub) CNTs juga telah dikaji. Hasil kajian menunjukkan bahawa jenis sumber karbon boleh mempengaruhi mekanisme pertumbuhan CNTs. Mekanisme pertambahan gelang telah digunakan untuk menerangkan penghasilan CNTs daripada benzena. Mekanisme pertumbuhan CNTs daripada benzena adalah berbeza dengan mekanisme penguraian daripada metana. Oleh yang demikian, SWCNTs dengan diameter yang lebih kecil dan bermutu tinggi dihasilkan daripada penguraian metana berbanding SWCNTs yang dihasilkan daripada benzena. Selain itu, CNTs yang dihasilkan daripada benzena mengandungi peratusan CNTs metalik yang lebih tinggi berbanding CNTs yang dihasilkan daripada metana.

SYNTHESIS OF SINGLE-WALL CARBON NANOTUBE VIA CVD GROWTH MECHANISM

ABSTRACT

Single-wall carbon nanotubes (SWCNTs) have been produced and studied since 1993 by many researchers. One of the challenges is to establish ring addition mechanism for a wide range of reaction temperature. By doing this, the growth mechanism of SWCNTs synthesised from aromatic hydrocarbon can be fully understood. Thus, this became the priority concern of this work. This work was started with the development of a catalyst system which was able to form the highest quality of SWCNTs from decomposition of methane. Response surface methodology (RSM) was applied to optimise the reaction parameters such as reaction temperature, reaction time and reaction gas flow rate. The optimum conditions was determined to be a reaction temperature of 900°C, a reaction time of 59 min and a reaction gas (methane/nitrogen) flow rate of 54 mL/min. The effect of carbon precursors on carbon nanotube (CNT) formation was studied. The results show that the types of carbon precursors greatly affect the quality of CNTs produced. Ring addition mechanism was used to explain the formation of CNTs from benzene. The ring addition mechanism for benzene is different with the growth mechanism of CNTs from methane. Due to this reason, smaller diameter and better quality of SWCNTs was formed from decomposition of methane compared to SWCNTs produced from benzene. Besides, it is also found out that higher percentage of semiconducting CNTs was synthesised from methane compared to benzene.

CHAPTER 1

INTRODUCTION

1.1 Nanomaterials

Over the past decade, nanomaterials are one of the topics of intense interest among the researchers. They have the great potentials for electronic, biomedical and industrial applications due to their excellent properties such as mechanical and electrical. A large amount of fund has been channeled into nanomaterials research by private enterprise and government to develop and advance this field further as well as meeting the demand from industries.

Nanomaterials have been referred to materials whose size of elemental structure has been produced at least in one dimension in the nanometer scale (1-100 nm). “Nano” word is comes from a Greek word meaning dwarf or extremely small. One nanometer spans 3-5 atoms lined up in a row. Although the interest in nanomaterials started a decade ago, the concept was raised over 40 years ago. Physicist Richard Feynman delivered a talk in 1959 entitled "There's Plenty of Room at the Bottom", in which he commented that there were no fundamental physical reasons that materials could not be made by maneuvering individual atoms. Actually, nanomaterials have been produced and used by human since hundreds of years ago. As an example the beautiful ruby red color of some glass is because of the gold nanoparticles trapped in the glass matrix. The decorative glaze known as luster, found on some medieval pottery, contains metallic spherical nanoparticles dispersed in a complex way in the glaze, which give rise to its

special optical properties. The techniques applied to fabricate these materials were kept in secret at that time and are unknown until now.

Development of nanotechnology has been spurred by the invention of high resolution transmission electron microscope (HRTEM) and scanning tunneling microscope (STM) to observe object in nano size. By 1990, scientists at IBM used STM probes to position individual xenon atoms to spell out IBM logo. In 1980, fullerene C_{60} was discovered and inspired research that led to production of carbon nanofibers (CNFs) with diameters under 100nm. Later in 1991, the first single-wall carbon nanotube (SWCNT) was discovered by Iijima (1991) using the HRTEM in NEC laboratory, which are now produced by many companies in commercial quantities. By 1999 the world market for nanocomposites grew to millions of dollars and is still growing fast. Nanomaterials are appearing in many types and their applications are range from electrical, biomedical, military and automobiles.

1.2 Carbon nanotubes

Before Sumio Iijima (1991) discovered the carbon nanotubes (CNTs), diamond, graphite and fullerene are carbon materials that possess almost similar structure to CNTs. Graphite is formed by few planar layers of hexagonal carbon atom which is bound by sp^2 -type bonds. Each layer is bound by weak van der Waals force. However, in diamond, sp^3 -type bonds bind each of carbon atoms at the apexes of a tetrahedron. In fullerene (C_{60}), the bonds between carbon atoms are hybridized sp^2 -type. There are 60 carbon atoms which bound into a soccer ball-type structure involving a combination of 20 hexagon rings and 12 pentagon rings. The shape of the fullerene is spherical because

of the non-aromatic of hexagonal rings. The positions of both single and double bonds of the hexagonal rings in fullerene are interacting with the pentagon rings. As a result, hexagonal rings do not resonate unlike the aromatic hexagonal rings in graphite and benzene which consist of resonant single and double bonds.

The basic structure of SWCNTs are hexagonal carbon rings which bound by hybridized sp^2 -type bonds. These bonds form a helical array of aromatic hexagonal rings of carbon on a seamless cylindrical graphene shell. The diameters are range from 0.1-2 nm and the lengths can range from few nanometers to microns. The ends of SWCNTs are capped by fullerene hemispheres and called as fullerene nanotubes (Figure 1.1) (Yakobson and Smalley, 1997), are actually hybrid structures. Multi-wall carbon nanotubes (MWCNTs) are made up from several layers of graphene whose helical pitches are different from one another. The ends of MWCNTs are also capped by fullerene hemisphere.

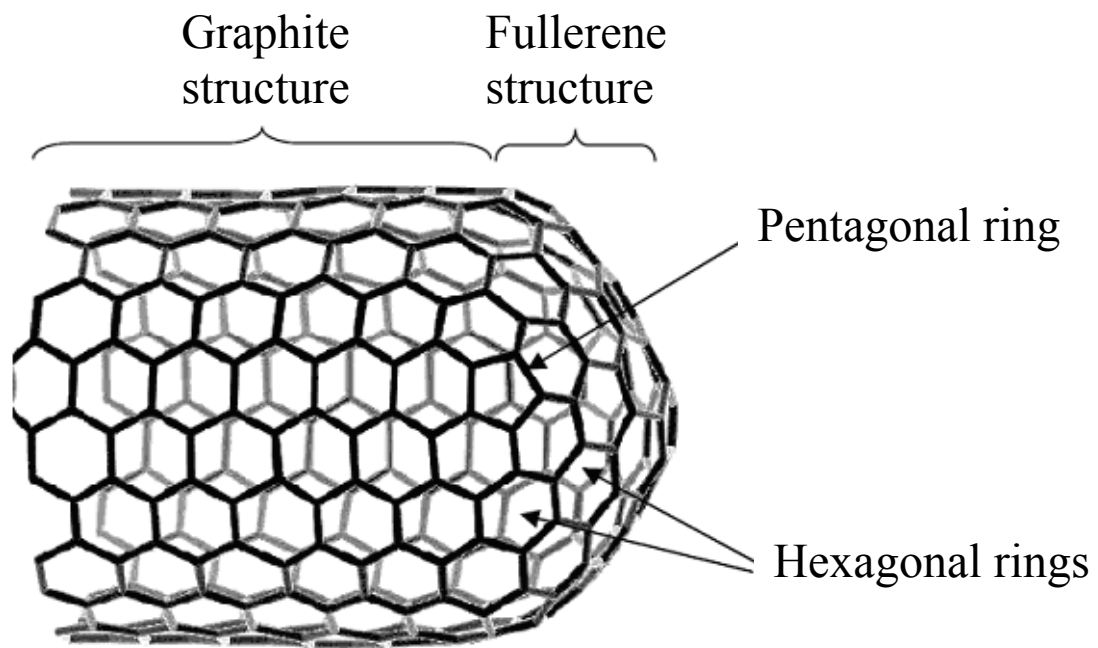


Figure 1.1 The structure of SWCNT (Nanodimension, 2005).

Before the discovery of CNTs by Iijima, scientists had been investigating the synthesis and properties of carbon filaments. They invented electron microscope to observe nanosize of carbon filaments (Davis *et al.*, 1953). The diameter of carbon filaments are range from 10 to 100nm and produced by the pyrolysis of carbon dioxide and hydrocarbons, were observed possess hollow cores (Oberlin *et al.*, 1976, Tibbetts, 1984). CNFs synthesised by chemical vapour deposition (CVD) are identified as carbon filaments thickened by deposited carbon and that at the core is a CNTs (Biro *et al.*, 2001). It is likely that CNTs have been produced by the scientists who had been producing carbon filaments.

1.3 Synthesis of SWCNTs

Since Iijima and Ichihashi (1993) discovered SWCNTs using arc-discharge technique, SWCNTs have been produced by using other techniques such as CVD and laser ablation until now. The first production of high quality and milligram amounts of SWCNTs (Thess *et al.*, 1996a, Bethune *et al.*, 1993) marked the important milestones that enabled the study of the intrinsic properties of SWCNTs. CVD for high quality and yield of SWCNTs (Dai *et al.*, 1996, Hafner *et al.*, 1998, Kong *et al.*, 1998b) further opened up new routes for controlled production and device integration. It is obvious that highly improved and controlled production of SWCNTs can help the developments for CNTs based science and technology in future. SWCNTs are available in the market now. They are categorized into functionalised (OH and COOH), short and functionalised short SWCNTs with 90% purity. Separated semiconducting and metallic SWCNTs are

available as well for commercial. This indicates that several types of SWCNTs with high quality can be produced from chemical treatment on the raw CNTs samples.

1.4 Growth mechanism of SWCNTs

As the applications for SWCNTs range from nanoelectronics and field emitters to composite materials, reliable growth techniques for high purity and yield of SWCNTs are crucial in order to utilise SWCNT's potential. The growth mechanism of SWCNTs has been the topic of much conjuncture in the literature; despite this, however, the actual growth mechanism is still remaining not fully understood. One of the popular growth mechanism of SWCNTs is similar to the growth mechanism of carbon filaments proposed by Baker (Dupuis, 2005, Loiseau *et al.*, 2006). The growth mechanism of carbon filaments generally adopted is based on the concepts of the VLS (vapor-liquid-solid) theory developed by Wagner and Ellis (Loiseau *et al.*, 2006, Dupuis, 2005). Based on the growth mechanism of carbon filaments, there are four steps to be considered. The four steps are diffusion of carbon precursor species to the catalyst surface, decomposition of carbon precursor into carbon atoms, diffusion of carbon atoms through the catalyst nanoparticles to another sites, and segregation and bonding of carbon atoms to form carbon layers (Loiseau *et al.*, 2006, Dupuis, 2005). However, the further explanation on the formation of carbon layers was not explained by growth mechanism of carbon filament. Thus, Yarmulke mechanism was proposed by Dai *et al.*, (1996) to explain it. According to Yarmulke mechanism, a nanoparticle exhibits very high surface energy problem on a per atom basis. The formation of a carbon layer which is called graphene on nanoparticles can help to solve this problem by reducing the very high

surface energy. It is because the basal plane of graphene has a very low surface energy, thus, the total surface energy of nanoparticle can be decreased. Even though both Yarmulke and carbon filaments growth mechanism can elucidate the growth mechanism of CNTs, but one question still remains is whether these growth mechanism can be applied on all types of carbon precursors. Few years later, Tian *et al.*, (2003) proved that when benzene was used as carbon precursor, ring addition mechanism involved. According to ring addition mechanism, benzene ring is the basic building block for the formation of CNTs. Later on, this ring addition mechanism was proved again by Kumar and Ando (2003c) when camphor was used as carbon precursor to produce SWCNTs. It is clear that the growth mechanism of SWCNTs is cannot be explained by a single model growth mechanism. It is because there is a gap between the growth mechanism and synthesis of SWCNTs. This implies that the understanding on the growth mechanism is merely superficial. This explained the reason why the chirality of SWCNTs cannot be controlled by any scientist until now. Today, this gap is become much smaller compared to twenty years ago. For instance, impurity-free SWCNTs is able to produce using water-assisted CVD (Hata *et al.*, 2004). Currently, high-pressure catalytic decomposition of carbon monoxide (HiPCO) (Nikolaev *et al.*, 1999) is used by Smalley's research group at Rice University and it is the only CVD method that can produce SWCNTs on a kilogram per day scale. Besides, plasma-enhanced CVD (PECVD) methods have been widely used for producing high-quality SWCNTs and reported by some research groups (Li *et al.*, 2005, Zhong *et al.*, 2005, Zhang *et al.*, 2005, Wang *et al.*, 2006, Kato *et al.*, 2006).

1.5 Problem statement

Research in the SWCNT field has moved to the level where a good understanding of the structure and of many of the basic properties has been achieved. Some of the unexpected theories that do not possessed by graphite have been discovered in nanotubes, and these discoveries have generated great motivation not only in nanotube research, but also nanoscience research in general. On the other hand, the lack of a detailed understanding of the nanotube growth mechanism such as ring addition mechanism still remains until now. Such an understanding is very important because of the very close connection between nanotube properties and their geometric structure. With this understanding, the diameter and chirality of nanotube can be controlled by chemical synthesis method.

From the beginning of discovery of SWCNTs, the main focus of SWCNT research has been in the synthesis area, and this remains the great challenge of the field. Rapid progress is being made to increase control of the synthesis process, narrowing the diameter and chirality range of the nanotubes, reducing defects and impurities and increasing production efficiency and yield while expanding nanotube functionality.

To date, good quality and nearly uniform diameters of SWCNTs have been synthesised successfully by many researchers and their works have been published in some high impact factors journals. However, complicated catalyst preparation and sophisticated equipments are involved to produce a small amount of SWCNTs. Moreover, high reaction temperature (900-1100°C) is needed to form SWCNTs (Ago *et al.*, 2001, Bonadiman *et al.*, 2006). Therefore, the cost of SWCNT production has been increased. Cantoro *et al.*, (2006a) reported that they were able to produce SWCNTs as

low as 350°C. Hata *et al.*, (2004) used the water-assisted CVD method to synthesise impurity-free SWCNTs with heights up to 2.5 mm. However, Si(100) wafers which is an expensive material, were used as substrates and sophisticated equipments were used as well. With these factors, the cost of large scale SWCNT production becomes a large amount.

It is known that chirality of SWCNTs determined the mechanical and electrical properties (Saito *et al.*, 1998, Dai, 2002a). However, mixtures of SWCNTs, MWCNTs and other impurities are usually produced when using normal methods. They are difficult to separate by type, length, diameter or any other characteristic (Krupke and Hennrich, 2005). The cost of purification by chemical method to remove all impurities are high and involves many steps (Tan *et al.*, 2008). Therefore, knowledge of the growth mechanism is very important to be established so that the SWCNTs with desirable properties can be synthesised (Beuneu, 2005, Little, 2003).

The growth mechanism of SWCNTs is still a popular debate topic (Reilly and Whitten, 2006) which is due to the many types of carbon precursors and different reaction conditions have been used in CVD to form CNTs. There are several parameters in CVD that can be controlled such as reaction temperature, reaction times, gas flow rate and the type of carbon precursor. The type of active metal and support also influences the growth of SWCNTs.

Many elementary steps are involved in the formation of SWCNTs (Eres *et al.*, 2005). The elementary steps are decomposition of carbon precursor into carbon atoms, deposition of carbon atoms on the catalyst surface, diffusion of carbon atoms through the catalyst nanoparticles and formation of graphene cap on the catalyst surface for producing SWCNTs. If a particular growth mechanism is supported by strong

experimental evidence, then that growth mechanism can only be applied to these experimental conditions. For instance, when benzene was used as carbon precursor, the growth mechanism of CNTs is affected by molecular structure of benzene which is different from the growth mechanism of CNTs produced by methane. The root of this problem is the insufficient of proper understanding of the SWCNT growth mechanism. Till date, a general growth mechanism that can explain all observed growths occurring under different conditions during CVD has not been established. There are several issues in the growth mechanism that are yet to be clarified. In this work, one specific problem has been focused: the question of whether different molecular structure of carbon precursors influences the growth mechanism and quality of SWCNTs. Thus, the vital parts of present work are to find out and study the way of SWCNT grow and obtaining the controlled synthesis using a simpler method.

1.6 Research objectives

- 1) To develop a catalyst system that can synthesise high quality of SWCNTs by studying the effect of various catalyst supports and active metals, and the effect of metal loading on methane decomposition into SWCNTs.
- 2) To optimise the operating parameters (reaction temperatures, reaction times and gas flow rates) in the SWCNT production using response surface methodology. This is followed by analyzing, modeling and optimising numerically to generate optimum conditions.
- 3) To study the influence of molecular structure of methane, benzene and camphor on the growth mechanism and quality of SWCNTs.

1.7 Scope of the study

The present study mainly focuses on catalyst development, optimisation SWCNT synthesis and growth mechanism study for SWCNTs. The CVD is carried out at atmospheric pressure in a vertical fixed-bed quartz reactor. The freshly prepared Fe₃O₄/MgO catalysts are characterised using scanning electron microscope (SEM), transmission electron microscope (TEM) and X-ray diffractometer (XRD). After CVD, the black colors of catalysts are characterised using XRD, SEM, TEM, thermogravimetric analysis (TGA), Raman spectroscopy.

The objective of catalyst development is to develop a catalyst system that shows highest catalytic activity in producing high quality of SWCNTs. From literature, nickel (Seidel *et al.*, 2004, Colomer *et al.*, 1999, Colomer *et al.*, 2000), cobalt (Satishkumar *et al.*, 1998, Marty *et al.*, 2002, Colomer *et al.*, 1999, Colomer *et al.*, 2000) and iron (Cheng *et al.*, 1998a, Nikolaev *et al.*, 1999, Li *et al.*, 2001, Cheung *et al.*, 2002) are the popular active metals that have been used to form SWCNTs. Silicon oxide, magnesium oxide and alumina are the good catalyst supports by providing strong interaction with active metals. One catalyst system only will be chosen to be used in the optimisation of experimental conditions and SWCNT growth mechanism study. Optimisation of experimental conditions and SWCNT growth mechanism study using bimetallic catalyst system has been widely reported; however, application of single metallic catalyst system to the production of SWCNTs is rare. Therefore in this project, three types of active metals and catalyst supports are tested.

In the optimisation SWCNT synthesis, three variables: reaction temperatures, reaction times and gas flow rate are chosen. These variables are selected because they

are reported to have effects on the carbon weight and the quality of SWCNTs. Response surface methodology (RSM) is used to develop the models and the most influential factors in each experimental design-response is identified using the analysis of variance. This is followed by the determination of the optimum reaction conditions numerically from the whole set of experimental data.

Lastly, two types of carbon precursors are used to synthesise CNTs from 600-1000°C. The gas in the reactor during CVD is collected for all experiments and further analysed by gas chromatography mass spectrometry (GCMS). The morphology of samples produced by different types of carbon precursors are compared after characterized by using TEM, SEM and Raman. From the data collected, the growth mechanisms of CNTs are studied at different reaction temperatures synthesised by different carbon precursors. The diameter distributions of SWCNTs produced from benzene and methane are investigated. The method to calculate the percentage of metallic and semiconducting SWCNTs in a sample is discussed before the end of chapter.

CHAPTER 2

LITERATURE REVIEW

2.1 Introduction of carbon nanotubes

2.1.1 Discovery of carbon nanotubes

It is known that carbon is the most versatile element that exists on the earth. Carbon has been used to reduce the metal oxides for more than 6000 years. Graphite and diamond are two different forms of carbon which were discovered in 1779 and 1789, respectively. After 200 years, a new form of carbon called fullerene was discovered by Harold Kroto, Richard Smalley and Robert Curl (Kroto *et al.*, 1985). A few years later the CNTs were discovered. Carbon nanotubes (CNTs) were first discovered in 1991, by Sumio Iijima in fullerene soot (Iijima, 1991). The same method to produce fullerene was used to form CNTs. In this CNTs form, carbon atoms were arranged in a tubular shape to form cylindrical nanostructure. High resolution transmission electron microscopy (HRTEM) was used to observe CNTs. The structure of CNTs is different with the carbon fibres which consists of coaxial cylinders of 2 to 50 graphite sheets (Yamabe, 1995). The first CNTs discovered by Sumio Iijima was MWCNTs (Iijima, 1991) and after two years, he produced single-wall carbon nanotubes (SWCNTs) (Iijima and Ichihashi, 1993). Iijima and Ichihashi (1993) used two carbon electrodes with 20V d.c. current generated between of them in a methane and argon filled carbon-arc chamber to form SWCNTs. In the same year, Bethune *et al.*, (1993) also produced SWCNTs using arc-discharge technique. In 1996, Smalley synthesised bundles of SWCNTs for the first

time (Thess *et al.*, 1996b). The name carbon nanotube (CNT) is derived from their size which is only a few nanometers wide.

Before the invention of CNTs by Sumio Iijima in 1991, the journal Carbon has suggested that the first report of nanoscale carbon fibres with hollow internal cavities, which the editors equate with CNTs, was in 1952 (Monthieux and Kuznetsov, 2006). The editorial mentioned that the structure of concentric layers of carbon that similar to the properties of MWCNTs was observed in 1958. Although CNTs were produced before 1991, their properties were not understood until Sumio Iijima related their structure to fullerenes. Figure 2.1 shows the structure of fullerenes. The discovery of fullerenes (Figure 2.1) (Kroto *et al.*, 1985) had encouraged many researchers to study the properties of closed-cage carbon structures. Indeed, there were some theoretical investigations that described the properties of extended fullerene-like molecules, which were carried out before Iijima's work (Saito *et al.*, 1998, Monthieux and Kuznetsov, 2006, Kroto *et al.*, 1985, Mintmire *et al.*, 1992, Dresselhaus *et al.*, 1992). Without the discovery of fullerenes, the amazing properties and structures of nanotubes may never have been explored.

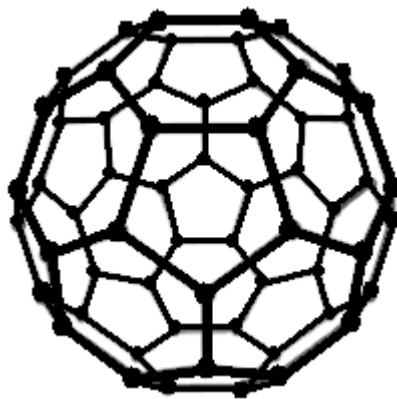


Figure 2.1 Structure of the buckminsterfullerene (C₆₀).

2.1.2 Structure of CNTs

Carbon atoms can be arranged in different orders (sp , sp^2 and sp^3) which allow them to form variety of carbon materials (Cotton *et al.*, 1999, Greenwood and Earnshaw, 1998). Figure 2.2 shows the structure of graphite and diamond. Diamond and graphite are the two well-known allotropes of carbon. Graphite is a flat sheet of carbon atoms. Each of the carbon atoms is sp^2 hybridized, and the σ -bonding using the sp^2 orbitals between neighbouring carbon atoms to form a network of hexagons. The p orbitals on the carbon atoms form an extended π system that allows graphite to conduct. This is in contrast to the other well-known allotrope, diamond, where the carbon atoms are all sp^3 hybridized and bonded to four other carbon atoms in a tetrahedral arrangement.

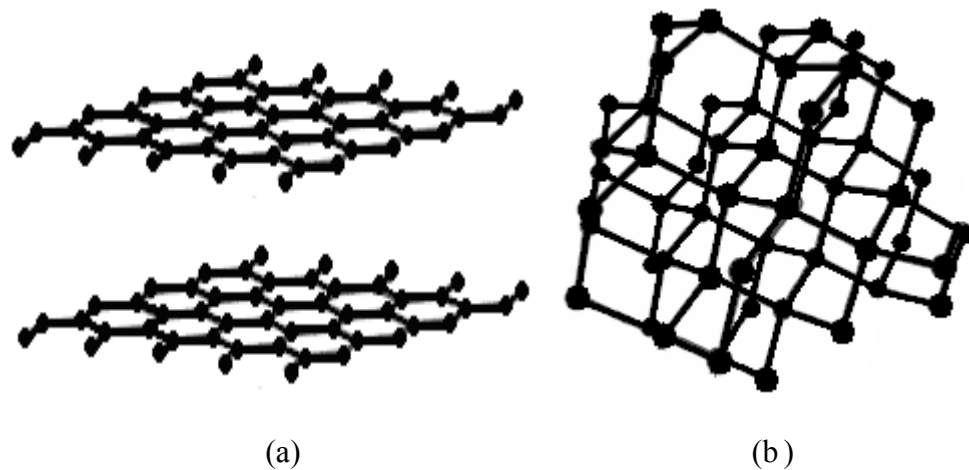


Figure 2.2 The structure of (a) graphite, (b) diamond.

The basic structure of a CNT is quite close to graphite. Graphene is made up of a single and seamless sheet of graphite. Figure 2.3 shows the CNT produced by rolling up a graphite sheet. The structure of a CNT can be conceptualised by wrapping a single layer of graphene into seamless cylinder so that its length is a million times (Dai,

2002a). One of the ends of the nanotubes is found either closed with a fullerene-like structure or open. Due to this kind of structure, some researchers described nanotubes as extended fullerenes.

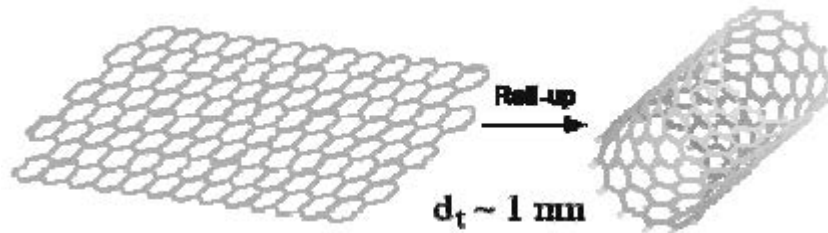


Figure 2.3 CNT formed by rolling up a graphite sheet (Andrews, 2006).

There are three classes of CNTs: single-wall, multi-wall and double-wall CNTs. Figure 2.4 shows the structures of SWCNTs, double-wall CNTs (DWCNTs), and multi-wall CNTs (MWCNTs). A single graphene rolled-up would form a SWCNT, two graphenes rolled-up would give a double-wall CNT and several graphenes that are rolled-up would produce a MWCNT.

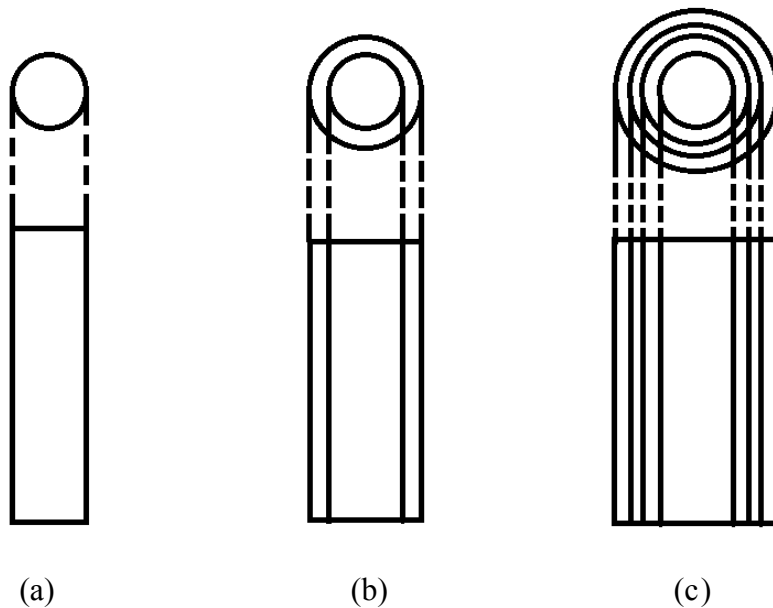


Figure 2.4 Structures of (a) single-wall, (b) double-wall, (c) multi-wall CNTs (Burstein, 2003).

The diameter of SWCNTs are usually found less than 2 nm whereas MWCNTs can be much larger in diameter but less than 100 nm (Harris, 1999). Mostly bundles of SWCNT are formed due to the van der Waals forces and π -stacking (Dyke and Tour, 2004). SWCNT can be formed in many different structures because a graphene can be rolled-up in many different ways. A SWCNT can be grown centimeters in length (Huang *et al.*, 2003). They possess large aspect ratio as they have very small diameter of around 1 nm. Because of this properties, they are quasi-one dimensional system and attracted many scientists (Dai, 2002b). CNTs have been used as model system to study the quantum phenomena of 1-D solids (Dai, 2002b).

2.1.3 Properties and application of carbon nanotubes

Since the discovery of CNTs in 1991, CNT properties have been studied and their potential applications are the most concerned by scientists. Electrical property is one of the most striking features of CNTs that has been studied details. As a result of the 1 dimensional nature of CNTs, electrons can be conducted in nanotubes without being scattered. The lack of scattering of the electrons is known as ballistic transport and allows nanotube to conduct without disperse energy as heat (Frank *et al.*, 1998). Experimental and theoretical results show excellent electrical properties of CNTs. They can carry current with capacity 1000 times higher than the copper wires (Collins and Avouris, 2000). For 1D system cylindrical surface, translational symmetry with a screw axis could affect the electronic structures and related properties. It was reported that the electronic characteristics possessed by CNTs are resulted from the interlayer interactions

rather than from interaction between different CNTs (Dresselhaus *et al.*, 1995). The electrical properties of a nanotube can be determined from the chiral vector (Avouris, 2002). If $(n-m) = 3q$ where q is an integer, the tube is metallic, otherwise the tube is semiconducting. The band-gap (E_g) of semiconducting tubes has been seen to be inversely proportional to the diameter of the tube (Avouris, 2002). The band-gap energy decreases as the tubes increase in diameter, as they accumulate graphite, which is a zero band-gap material (semi-metal).

Due to the small diameters of CNTs and unique electrical properties, much attention has been concentrated in using nanotubes as electronic devices (Ouyang *et al.*, 2002, Avouris, 2002). It is hoped that with this properties, electronic devices like transistor that will use less energy and release less heat can be produced. One of the most popular designs of nanotube transistor is the field effect transistor (FET). However, the application of CNTs in electronics still faces many obstacles such as difficulty to make reliable contacts with other materials (Dai, 2002b). As FETs can be produced using semiconducting nanotubes only (Avouris and Chen, 2006), CNT samples contain mixture of semiconducting and metallic CNTs still is a problem that remains until now. Moreover, it is difficult to separate nanotubes by their electrical characteristics (Krupke and Hennrich, 2005).

Because of CNTs have good conductivity and narrow diameters, they possess good electron-emission properties (Rinzler *et al.*, 1995). When a nanotube is attached to a cathode, its narrow diameter and high aspect ratio will produce large electric fields at the tip of the nanotube, therefore electrons will be easily emitted (Xu and Huq, 2005). Vertical aligned CNTs will be suitable to be used as electron emission gun in fabricating devices such as flat panel displays (Jamieson, 2003).

CNTs also have very good thermal conductivity since being a good electric conductor. The thermal conductivity of a SWCNT can achieved as high as $6600 \text{ Wm}^{-1}\text{K}^{-1}$ at room temperature (Berber *et al.*, 2000). The network structure and strong bonds possessed by diamond, make it becomes one of the best thermal conductors (Berber *et al.*, 2000), has a thermal conductivity of $1000 \text{ Wm}^{-1}\text{K}^{-1}$ at 0°C (Linde, 2006)

CNTs are predicted to have high stiffness and axial strength as a result of the carbon-carbon sp^2 bonding (Popov, 2004). Experimental and theoretical results have shown an elastic modulus of greater than 1 TPa (elastic modulus of diamond = 1.2 TPa) and have reported strength 10-100 times higher than the strongest steel at a fraction of the weight (Thostenson *et al.*, 2001). Due to high in-plane tensile strength of graphite, both SWCNTs and MWCNTs, are expected to have large bending constants since they mostly depend on Young's modulus. Simulations conducted on SWCNTs indicate that deformation of SWCNTs related directly to an abrupt release in energy and a singularity in the stress/strain curve. SWCNTs were found to have an extremely large breaking strain which decreased with temperature. The elastic modulus, Poisson's ratio and bulk modulus were all found to be directly affected by the nanotube radius. However, the properties of MWCNTs were complicated to calculate. An empirical lattice dynamics model shows that MWCNTs were insensitive to parameters such as the chirality, tube radius and the number of layers (Thostenson *et al.*, 2001).

CNTs have low densities compared to other strong materials like steel. Bernholc *et al.*, (1998) found that nanotube can regain its original shape after twisted or bent from the computer simulation. Its "kink-like" ridges allow the structure to relax elastically while under compression, unlike carbon fibers which fracture easily (Thostenson *et al.*, 2001). This is because CNTs are flexible perpendicular to the tubes axis and become the

interest of researchers in trying to produce new strong materials, especially in making polymer composites (Jamieson, 2003, Dyke and Tour, 2004). CNTs have been used to enhance the mechanical properties of polymer composite by increasing the Young's Modulus and tensile strength (Qian *et al.*, 2000). However, CNTs are not easy to disperse in polymer (Dyke and Tour, 2004). This is due to the little adhesion between the polymer and the nanotubes (Dyke and Tour, 2004). Therefore, the strength of composites is not increased and even worse compared to the pure polymer. To solve this problem, nanotubes have been added with functionalised group to make them easier to disperse in polymers and to increase the adhesion of nanotubes and polymer by creating covalent bonds between them (Dyke and Tour, 2004). This approach may damage the nanotubes because it can cause disruption to the nanotubes structure. Then, nanotubes may lose its functionality to increase mechanical properties of composite (Dyke and Tour, 2004).

CNTs are known as material that possess high surface area and the internal cavities of nanotubes can store hydrogen as an energy source (Ning *et al.*, 2004). This provides a way to store hydrogen and transported it safely and economically for certain applications (Cheng *et al.*, 1998b). However, due to the inconsistency of quality for the produced CNTs, there now seems to be a little hope to use CNTs as hydrogen storage widely (Cheng *et al.*, 2001).

Even though CNTs possess some great properties, there is one challenge faced by scientists before they can apply CNTs in a new product. The challenge is how to control the chirality of CNTs to produce either semiconducting or metallic SWCNTs. Thus, the understanding for the growth mechanism of SWCNTs is very important and the growth mechanism of SWCNTs will be studied in this work.

2.2 Synthesis of carbon nanotubes

2.2.1 Arc-discharge

Figure 2.5 shows the setup of arc-discharge. Arc-discharge was first used by Iijima (1991) to synthesise CNTs. The experimental setup and conditions are same with those applied for production of fullerenes. This technique involves placing two graphite electrodes close to each other's about 1 mm in an atmosphere of inert gas like helium at a pressure of 500 torr (Harris, 1999). An arc occurs between the electrodes when a voltage of 20-25 V with a current of 50-120 A is applied. The temperature is very high in the chamber and evaporates carbon from the electrodes. This arc-evaporated material then re-condenses on the cathode, and the subsequent deposit contains CNTs. SWCNTs were produced by doing the electrode with metals such as Ni, Fe, Co, Gd and Y (Saito *et al.*, 1998). The disadvantage of this technique is carbon impurities and encapsulated nanoparticles are usually produced beside CNTs (Harris, 1999). Short CNTs are tending to be produced as well. However, the advantage is both of SWCNTs and MWCNTs are easily to be synthesised and moderate cost production is needed.

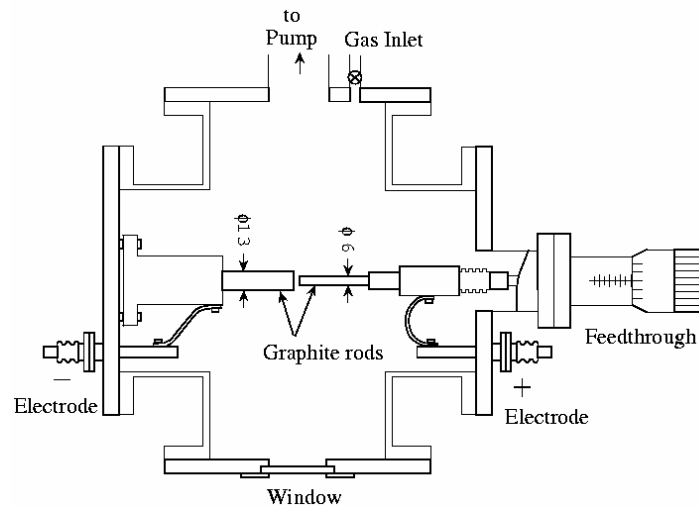


Figure 2.5 A diagram of arc-discharge setup (Saito *et al.*, 1998).

2.2.2 Laser ablation

This technique operates at same conditions to arc discharge. A diagram of the experimental setup is shown in Figure 2.6. Both methods involve the condensation of carbon formed from the vaporization of graphite. When target doped with metals such as Ni, Co and Pt, SWCNTs are formed. In this technique, the graphite target is placed in a quartz tube surrounded by a furnace heated at 800-1500°C. A 500 torr of argon gas is passed through the tube to carry the soot formed to a water-cooled Cu collector. The advantage of this technique is favours the production of bundles SWCNT. Amorphous carbon and encapsulated nanoparticles are also produced in the end product. It has been claimed by Thess *et al.* (1996a) that high yields with more than 70-90% conversion of the graphite to CNTs are achieved with this technique. The disadvantage is the cost production is very high due to high power and expensive of laser is required.

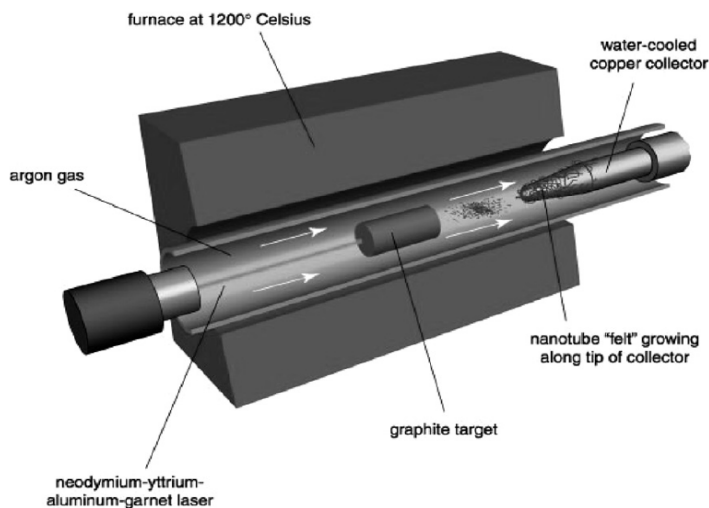


Figure 2.6 A diagram of laser ablation setup (Yakobson and Smalley, 1997).

2.2.3 Chemical vapour deposition

An experimental setup of CVD is shown in Figure 2.7. In this technique, metal catalysts are used to crackdown the molecules of carbon sources to synthesise CNTs (Little, 2003, Moisala *et al.*, 2003, Dupuis, 2005). A supported catalyst is heated in a furnace to 600-1000°C together with hydrocarbon gas for a period of time (Moisala *et al.*, 2003). The carbon sample is then allowed to cool down in an inert gas environment to avoid etching away the CNTs by reaction with oxygen. MWCNTs are mainly formed at lower temperatures (300-800°C), whereas SWCNTs require higher temperatures (600-1000°C). Many types of carbon sources such as methane, benzene, camphor, ethanol, ethane, alcohol, carbon monoxide, hexane, cyclohexane, naphthalene, anthracene and others have been used to produce CNTs (Li *et al.*, 2004a). For the synthesis of SWCNTs, carbon monoxide and methane has been found to be effective (Moisala *et al.*, 2003). The most popular metals used to produce CNTs are iron, nickel, cobalt and molybdenum (Moisala *et al.*, 2003). However, the combination of two metals is active to form CNTs, particularly mixtures of molybdenum with other metals. The most common metals such as silica, alumina and magnesium oxide are used as supports (Dupuis, 2005). The advantage of this technique is production of CNTs can be scale up and better control over the growth of CNTs due to the greater scope for controlling reaction conditions, such as designing catalysts (Dupuis, 2005, Dai, 2002b). However, the disadvantage is mixture of SWCNTs and MWCNTs are produced together during the CVD.

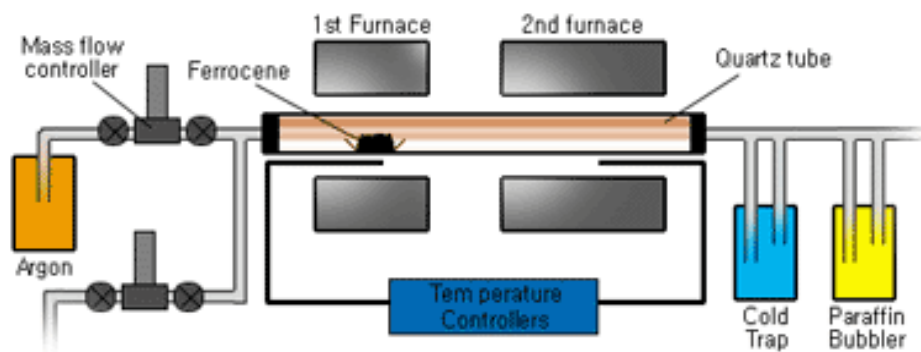


Figure 2.7 A diagram of CVD setup (Lee *et al.*, 2002).

2.3 Catalyst preparation methods

There are several types of transition metals and supports that can be mixed up to prepare a catalyst system. Various methods have been used to prepare catalyst and some are discussed in the following sections.

2.3.1 Sol-gel method

The sol-gel is a wet-chemical method in which the sol (or solution) evolves gradually towards the production of a gel-like material which contains of both liquid and solid phase. In this process, a precursor of the active component is mixed with the precursor of a textural promoter at given weight ratio between the two precursors. Textural promoter has been used to stabilise the active component structure preventing its sintered during the course of post treatments (Ermakova *et al.*, 2001). A hard-to-reduce oxide (HRO) such as silica or alumina has been used as textural promoters. To prepare the iron/silica nanocomposite particles, tetraethoxysilane (precursor of textural promoter) is mixed with iron nitrate (precursor of the active component) aqueous solution and ethanol. This is followed by the drying process to remove the water and

solvent and finally calcined (Pan *et al.*, 1999). Yeoh *et al.*, (2009) reported that the yield of CNTs can be increased to 354.3% by using the sol-gel method to prepare the Co-Mo/MgO catalyst. The sol-gel synthesis method has been reported to ensure a highly homogeneous distribution of transition metal in the matrix.

2.3.2 Coreduction of precursors

In the co-reduction process, the precursors are reduced simultaneously to form a new compound which is in oxide form. For instance, precursor such as $\text{Co}(\text{NO}_3)_2 \cdot 6\text{H}_2\text{O}$ or $\text{Fe}(\text{NO}_3)_2 \cdot 6\text{H}_2\text{O}$ and $\text{Mg}(\text{NO}_3)_2 \cdot 6\text{H}_2\text{O}$ were mixed with an organic compounds such as citric acid or urea and water (Chen *et al.*, 1997, Bacsá *et al.*, 2000, Pinheiro *et al.*, 2003). Then, the mixture was calcined to reduce the precursors to form mixed oxide particles.

2.3.3 Impregnation

In the impregnation method, a catalyst precursor e.g. ironoxalate (Ivanov *et al.*, 1994) will be dissolved in a solution to contact with a support. The precursor was deposited onto the support, and then solvent was removed by heating until the catalyst was dried (Venegoni *et al.*, 2002).

2.3.4 Ion-exchange-precipitation

In this preparation method, a solution of a catalyst precursor such as cobalt-acetate (Hernadi *et al.*, 1996) or cobalt-nitrate (Ivanov *et al.*, 1994) was supported by zeolite. An anion of the precursor was exchanged with an anion of the zeolite to form a new precursor molecule. The next step followed by calcination to form an oxide catalyst.